Gadoxetate Disodium (Gd-EOB-DTPA) Contrast Enhanced Magnetic Resonance Imaging Characteristics of Hepatocellular Carcinoma in Dogs

Chase Constant, Silke Hecht, Linden E. Craig, Cassie N. Lux, Claire M. Cannon, Gordon A. Conklin

From the Department of Small Animal Clinical Sciences (Constant, Hecht, Lux, Cannon, Conklin) and the Department of Biomedical and Diagnostic Sciences (Craig), College of Veterinary Medicine, University of Tennessee, Knoxville, TN 37996-4542

Dr. Cannon's current address is Department of Veterinary Clinical Sciences, College of Veterinary Medicine, University of Minnesota, St. Paul, MN 55108

Address correspondence and reprint requests to Dr. Hecht at shecht@utk.edu

Key Words: MRI, canine, liver, Eovist, Primovist, neoplasia

Running Head: MRI of Hepatocellular Carcinoma in Dogs

Funding sources: Funding provided by the ACVR Resident Research Grant

Previous Presentations or Abstracts: Portions of this study were presented at the ACVR Annual Scientific Meeting, October 7th-10th 2015, Minneapolis, MN

ABSTRACT

Hepatocellular carcinoma is the most common primary hepatic tumor in dogs and is amenable to surgical resection in many cases. Unfortunately, overlap of sonographic findings between benign and malignant hepatic lesions typically requires more invasive diagnostic tests to be performed (i.e. biopsy for histopathology). The availability of a non-invasive diagnostic test to identify hepatocellular carcinoma would be beneficial. The use of a liver-specific magnetic resonance imaging contrast agent such as gadoxetate disodium (Gd-EOB-DTPA; Eovist® or Primovist®) has improved lesion detection in human patients. In this descriptive study gadoxetate disodium contrast enhanced magnetic resonance imaging characteristics in dogs were evaluated in 7 dogs (total of 8 lesions). The imaging characteristics were variable with the exception of all lesions being hypointense to surrounding normal hepatic parenchyma on 3D T1-weighted gradient recalled echo images at all post-contrast time points. All lesions displayed signal intensity ratios less than 1, consistent with retained but impaired hepatocyte function. Hepatic lesions not identified on previous imaging were found in 3/7 patients which may affect surgical planning. In 2 patients several hepatic nodules were identified during surgery which had not been visualized on magnetic resonance imaging and were found to be benign on histopathology. This descriptive study reports the magnetic resonance imaging characteristics of hepatocellular carcinoma in dogs using the liver-specific contrast agent gadoxetate disodium.

INTRODUCTION

Hepatocellular carcinoma is the most common primary hepatic tumor in dogs, accounting for approximately 50% of reported tumors.[1,2] Three forms of hepatocellular carcinoma are recognized in dogs - massive, nodular, and diffuse. The massive form is the most common variant and may be amenable to surgical intervention.[1,2] The metastatic rate of

this form of the tumor is low (0-37%); however, local intrahepatic extension is possible making early diagnosis imperative for surgical treatment.[1-3] Abdominal ultrasound is routinely used to evaluate for hepatic disease, including tumors, in small animal veterinary patients.[4] Unfortunately, there is overlap of sonographic characteristics of benign and malignant hepatic lesions preventing accurate diagnosis without cytological or histopathological evaluation.[1,4,5,6] Additionally, well-differentiated hepatocellular carcinoma lesions can be difficult to differentiate from benign nodular regeneration based on cytology, requiring more invasive methods such a transcutaneous or surgical biopsy to be performed for the final diagnosis.[7] Other imaging modalities such as contrast-enhanced ultrasound[8] and computed tomographic angiography[9,10] have been evaluated in a limited fashion to characterize hepatocellular carcinoma in dogs. These studies have found certain imaging features useful in differentiating focal hepatic lesions; however, the clinical applicability of these techniques is currently limited by technical constraints, cost, and/or availability.[8,9,10] Improvements in detection and characterization of liver disease in canine patients by means of magnetic resonance imaging (MRI) could outweigh certain disadvantages (such as the need for general anesthesia, cost and study duration) due to its non-invasive nature compared to surgical or percutaneous sampling procedures, and due to optimization of staging, therapy planning, and prognostication.

Magnetic resonance imaging (MRI) is increasingly used in small animal veterinary patients, but reports of evaluation of hepatic lesions are limited.[11] The introduction of liver-specific MR contrast agents such as gadoxetate disodium (Gd-EOB-DTPA; Eovist® in the USA and Primovist® in Europe) in human medicine has shown an increased sensitivity for detection of hepatic lesions.[12] Gadoxetate disodium is a paramagnetic contrast agent that has 50% hepatobiliary and 50% renal excretion in healthy people.[13,14] It has proven safe for use in healthy dogs.[15] Reports of its use in dogs with hepatic disease are scarce.[16,17] A previous

study in dogs with focal hepatic lesions utilizing a low-field MRI system described 5 hepatocellular carcinoma lesions in 3 dogs and found good demarcation of the tumors which appeared hypointense compared to normal hepatic parenchyma on post contrast images.[16] The benefits of a high-field MRI system have been well-documented and include an increased signal-to-noise ratio which can increase lesion conspicuity and a decrease in duration of individual MRI sequences. Information about the gadoxetate disodium enhanced MRI appearance of canine hepatocellular carcinoma lesions using a high-field MRI system are lacking to date.

The purpose of this study was to describe the MRI characteristics of canine hepatocellular carcinoma lesions before and after administration of gadoxetate disodium using a high-field MRI system, determine the utility of MRI in identification of additional hepatic and extrahepatic lesions, and correlate MRI findings with surgical and histopathological results.

METHODS

This descriptive study was approved by the University of Tennessee Institutional Animal Care and Use Committee (IACUC). Eight client-owned dogs presented to the University of Tennessee College of Veterinary Medicine were prospectively enrolled when at least one hepatic mass was documented on previous abdominal imaging, owner permission for pre-operative MRI examination was given, and a subsequent final diagnosis of hepatocellular carcinoma was made based on histopathology from a surgical biopsy. The sample size was chosen based on similar descriptive studies in the veterinary literature. Each surgical biopsy was evaluated by a single board-certified veterinary pathologist (LEC). Decisions for inclusion or exclusion of patients were made by a veterinary radiology resident (CC) and a board certified veterinary radiologist (SH).

Magnetic resonance imaging (MRI) examinations were performed with a 1.5 Tesla magnet (MAGNETOM Espree™, Siemens Medical Solutions, Malvern, PA) and with patients under general anesthesia. Individual anesthetic protocols were determined for each patient by the on-duty anesthesiologist. Dogs were positioned in dorsal recumbency with a body flex matrix coil placed on the ventral abdomen. A standardized imaging protocol modified from a previous study was used for all dogs (Appendix 1).[15] Pre-contrast sequences performed on all dogs included T1-weighted spin echo and T2-weighted fast spin echo in the dorsal and transverse planes, T2*/T1 coherent gradient echo (TrueFISP; fast imaging with steady state precession) in the sagittal and dorsal planes, and T1-weighted 3D gradient echo (T1-W GRE; VIBE; volume-interpolated body examination) in the transverse plane. All dogs received 0.1ml/kg (0.025mmol/kg) of gadoxetate disodium (Eovist®, Bayer Healthcare Pharmaceuticals Inc., Wayne, NJ) administered intravenously as a manual bolus followed by 2ml of saline flush. Post-contrast sequences performed on all dogs included T1-weighted 3D gradient echo (T1-W GRE; VIBE) in the transverse plane acquired immediately and at 1, 5, 10, 15, and 20 minutes post-contrast administration, and T1-weighted fast spin echo with fat saturation in the dorsal and transverse planes at approximately 21 and 25 minutes post-contrast administration. Respiratory triggering or breath hold was not used for any sequence.

All images were jointly evaluated by a second-year veterinary radiology resident (CC) and a board certified veterinary radiologist (SH) using a commercial picture archival and communication system (SECTRA PACS IDS7™, Sectra Medical Systems AB, Linköping, Sweden), and a consensus was reached for subjective features. Investigators were aware of the final diagnosis in all dogs. Standard software tools were used to draw circular regions of interest (ROIs) and measure lesions with electronic calipers. Imaging characteristics recorded were pre- and post-contrast signal characteristics relative to normal liver parenchyma (hypointense, isointense, hyperintense), degree of heterogeneity (subjectively graded as: 0-

homogeneous, 1- mild heterogeneity, 2- moderate heterogeneity, 3- marked heterogeneity), lesion size (length, height, and width), and identification of other lesions (other hepatic lesions not seen on prior imaging modalities, enlarged hepatic lymph nodes and other extra-hepatic non-lymph node lesions). Additionally, signal intensity ratios (SIR) were calculated by the principal and mentoring investigators (CC and SH) from the pre-contrast and post-contrast T1-W GRE sequences at all time points to provide an objective measurement of degree of contrast enhancement between lesions and normal liver parenchyma. Analyses were performed in consensus. Signal intensity ratio was calculated using the following formula, which was modified from a previous study.[15]

SIR = Mean maximal signal intensity of hepatic lesion post contrast / maximal signal intensity of normal parenchyma post contrast.

The number of regions of interest (ROIs) drawn over hepatic lesions varied with the degree of heterogeneity to obtain a representative signal intensity, with 1 ROI drawn for homogenous lesion, 3 ROIs drawn for a mildly or moderately heterogeneous lesion and 5 ROIs for a markedly heterogeneous lesion. Degree of contrast enhancement was recorded on a 0-3 scale [0-none (SIR = 0), 1-mild ($0 < SIR \leq 0.5$), 2- moderate ($0.5 < SIR \leq 1.0$), 3-marked ($SIR > 1.0$)].

Subsequent to all MRI examinations, the dogs underwent exploratory laparotomy to evaluate the liver masses noted on MRI. When possible, partial or complete liver lobectomy was performed of liver masses suspected to be massive hepatocellular carcinoma, and the tissue was submitted for histopathology. Any remaining lesions of the liver noted on MRI or on gross examination and palpation of the liver were biopsied and submitted for histopathologic analysis.

Descriptive analyses were performed using commercially available software (Microsoft Excel®, Microsoft Corp, Redmond, Washington) by the principal and mentoring investigators (CC and SH). Means and standard deviations were calculated for normally distributed continuous data, and medians and ranges were determined for non-normally distributed data. Proportions were calculated for categorical data.

RESULTS

Eight dogs underwent abdominal MRI. One dog was excluded as the abdominal mass originally thought to be hepatic in origin based on abdominal ultrasound was in fact splenic in origin based on the MRI examination and surgery. In the remaining 7 dogs 8 hepatocellular carcinoma lesions were confirmed. The mean age of dogs was 11.6 +/- 1.3 years. There were six female spayed and 1 neutered male dogs. The median weight was 13.2 kg (range 7.7-29 kg). There were 2 mixed breed dogs and 1 each of the following breeds: Boston Terrier, Standard Poodle, Dachshund, Jack Russell Terrier, Border Collie and Yorkshire Terrier.

Mean study time from start to end of image acquisition was 50 +/- 2 minutes. The median size of the hepatic mass lesions was 9.35cm (2.1-10.5cm) in length, 7.3cm (1.8-11.2cm) in height and 7.55cm (1.9cm-11.0cm) in width. The MRI signal characteristics were variable and are summarized in Appendix 2. The only consistent signal characteristic between all lesions was hypointensity compared to normal liver parenchyma on post-contrast T1-W GRE sequences at all time points (Fig. 1). The degree of heterogeneity was variable with 3/8 (37.5%) lesions being markedly heterogeneous (grade 3), 2/8 (25%) being moderately heterogeneous (grade 2), 2/8 (25%) being mildly heterogeneous (grade 1), and 1/8 (12.5%) being homogeneous (grade 0). The majority of lesions, 7/8 (87.5%), displayed moderate contrast enhancement (grade 2). The remaining lesion (12.5%) displayed mild contrast enhancement (grade 1). The median maximal signal intensity ratio was 0.79 (range

0.5-0.98). Wash-in and wash-out characteristics for each lesion were determined by graphical analysis (Fig. 2). The majority of lesions (5/7) reached their lowest signal intensity ratio value (i.e. maximum difference between lesion enhancement relative to normal surrounding liver parenchyma) at 10 minutes post contrast medium administration.

Additional hepatic lesions, not identified on previous imaging studies, were identified on MRI in 3/7 (43%) of dogs. One additional mass was found in one dog (patient 7) in which only one mass had been seen on prior ultrasonographic examination. This second mass had similar MR characteristics as the other HCC lesions in this study and was confirmed as HCC on histopathology (see Fig. 1). One dog (patient 1) had multiple T2 hypointense nodules which showed very similar contrast medium uptake compared to normal liver and which were subsequently determined to represent vacuolar hepatopathy on histopathology (Fig. 3). In one dog (patient 5) two additional approximately 2 cm in diameter each masses not seen on ultrasound were found on MRI which showed imaging characteristics similar to the confirmed HCC lesion in this patient. However, as these lesions were located deep within liver lobes they were not identified in surgery, and sampling and histopathology were not performed. Enlarged hepatic lymph nodes were not identified in any dog. Non-lymph node extra-hepatic lesions were found in 2/7 (28.5%) of dogs. In one dog (patient 7) with a presumptive clinical diagnosis of abdominal wall lipoma the imaging characteristics of the mass were inconsistent with fat, and a diagnosis of soft tissue sarcoma was made subsequently. In another dog (patient 2) multiple splenic nodules of unknown etiology were noted. Finally, in 2 dogs several hepatic nodules were identified during surgery which had not been visualized on magnetic resonance imaging and were found to be benign on histopathology.

DISCUSSION

198 The MRI characteristics of hepatocellular carcinoma using the liver-specific contrast
199 agent gadoxetate disodium were variable in this sample of dogs. However, all lesions were
200 hypointense to isointense on pre-contrast T1-W GRE sequences and hypointense on post-
201 contrast T1-W GRE sequences at all time points which is similar to findings of a previous
202 study evaluating canine hepatic lesions using a low-field MRI system.[16] The degree of MRI
203 heterogeneity of the lesions in this study corresponded to histopathology, with two of the
204 grade 3 lesions (marked heterogeneity) being described as having multifocal areas of
205 hemorrhage and coagulative necrosis throughout and the third grade 3 lesion being described
206 as having lobules separated by fibrous bands. The one grade 0 lesion (homogeneous) had no
207 comment of hemorrhage, necrosis, or fibrosis tissue on histopathology.
208 Tumors in this study displayed contrast enhancement to a lesser degree than the
209 surrounding normal hepatic parenchyma. It has been shown in humans that gadoxetate
210 disodium distributes into the vascular and extravascular spaces following intravenous
211 injection.[13,14] Initially, this contrast agent has similar properties as non-organ specific
212 gadolinium-based contrast agents. However, over time the contrast medium is extracted by
213 hepatocytes primarily by organic anion transporter polypeptides, which are located at the
214 sinusoidal membrane.[13] The contrast medium is then excreted into the biliary tract via the
215 multidrug resistance-associated protein 2 at the canalicular membrane.[13] The same hepatocyte
216 transport mechanisms have been documented in rats.[18] To the authors' knowledge the exact
217 method of hepatobiliary excretion has not been confirmed in dogs but as the organic anion
218 transporter polypeptides and the multidrug resistance-associated protein 2 are similar to
219 people, a comparable method of hepatobiliary excretion of gadoxetate disodium is
220 assumed.[19,20] Changes in expression of these transporter proteins caused by carcinogenesis
221 results in variable contrast enhancement during the hepatobiliary phase in people.[13,21] In one
222 human study, it was determined that the expression of a transporter protein decreased with

223 increasing HCC grade which corresponded to a decrease in gadoxetate disodium
224 enhancement of lesions.[21] The signal intensity values determined in this study indicate that
225 canine hepatocellular carcinoma lesions have impaired but retained hepatocyte function,
226 although the exact changes to protein expression have not been evaluated in this species to
227 date. Time to maximum contrast enhancement of normal liver parenchyma and difference in
228 enhancement between normal liver and hepatocellular carcinoma was approximately 10
229 minutes in our patient population. This is similar to human studies and indicates that image
230 acquisition at this time point may optimize lesion detection and characterization.[22]
231 The identification of additional hepatic lesions not identified with other imaging is an
232 important clinical ramification as it may alter surgical planning. Abdominal ultrasound can be
233 limited in lesion detection, especially in larger patients and certain breed conformations. A
234 previous study has recommended the use of computed tomography evaluation of the
235 abdomen in patients greater than 25kg.[23] Of note, the patient with two hepatocellular
236 carcinoma lesions was the largest evaluated in this study and of deep chested conformation
237 (29kg; Border Collie) (see Fig. 1). The lesion not previously identified on abdominal
238 ultrasound was located in the craniodorsal aspect of the right lateral liver lobe, a region that
239 can be difficult to assess, emphasizing the benefit of cross-sectional imaging in assessment of
240 hepatic masses. One dog had two additional smaller masses identified on the MRI study, both
241 of which had imaging characteristics similar to the confirmed HCC lesion, although they
242 unfortunately could not be palpated during surgery, preventing a histopathologic diagnosis.
243 In 2 dogs the surgeon described multifocal small hepatic nodules noted during
244 laparotomy which had not been observed during MRI examination. In a 3rd dog hypointese
245 nodules were found on T2-weighted images which showed contrast medium uptake similar to
246 normal parenchyma and were not visible on post contrast images. Biopsies of these lesions
247 were consistent with nodular hyperplasia/vacuolar hepatopathy with no evidence of

malignancy on histopathology. Although the number of cases is too small to draw meaningful conclusions it is plausible that regenerative nodules and other benign liver lesions may have maintained function similar to normal liver parenchyma, resulting in a similar degree of contrast medium uptake as in normal liver parenchyma.

Limitations of this study include the small sample size of dogs and liver masses enrolled. Additionally, the regions of interest drawn over normal liver were not confirmed as normal on histopathology. However, no abnormalities were noted on ultrasound or MRI in the area of liver chosen as normal, and extensive biopsy sampling of presumably normal liver for confirmation was not possible in this population of client-owned dogs.

In conclusion, the imaging characteristics of gadoxetate disodium-enhanced MRI of canine hepatocellular carcinoma are variable. In this sample of dogs, all lesions were hypointense on post contrast T1-W GRE sequence, possibly indicating retained but impaired hepatocyte function. The MRI evaluations of the liver allowed for detection of additional hepatic and non-hepatic lesions not identified by abdominal ultrasound, affecting the clinical recommendations for these patients. Future studies comparing lesion detection and classification between gadoxetate disodium-enhanced MRI and non-organ specific contrast-enhanced MRI are required to establish the true benefit of this contrast agent.

LIST OF AUTHOR CONTRIBUTIONS

Category 1

(a) Conception and Design

Author name (s) Silke Hecht, Chase Constant

(b) Acquisition of Data

Author name (s) Chase Constant, Silke Hecht, Linden E. Craig, Gordon A. Conklin

(c) Analysis and Interpretation of Data

Author name (s) Chase Constant, Silke Hecht, Linden E. Craig, Cassie N. Lux, Claire M. Cannon

Category 2

(a) Drafting the Article

Author name (s) Chase Constant, Silke Hecht

(b) Revising Article for Intellectual Content

Author name (s) Chase Constant, Silke Hecht, Linden E. Craig, Cassie N. Lux, Claire M. Cannon

Category 3

(a) Final Approval of the Completed Article

Author name(s) Chase Constant, Silke Hecht, Linden E. Craig, Cassie N. Lux, Claire M. Cannon, Gordon A. Conklin

290 **REFERENCES**

291 1. Liptak JM. Hepatobiliary tumors. In: Withrow SJ, Vail DM, Page R (eds.): Withrow &
292 MacEwen's Small Animal Clinical Oncology. 5th ed. St. Louis: Elsevier, 2012;405-412.
293 2. Patnaik AK, Hurvitz AI, Lieberman PH, Johnson GF. Canine hepatocelluar carcinoma. Vet
294 Pathol 1981;18:427-438.
295 3. Elpiner AK, Brodsky EM, Hazzah TN, Post GS. Single-agent gemcitabine chemotherapy
296 in dogs with hepatoceullar carcinomas. Vet Comp Oncol 2011;9:260-268.
297 4. Nyland TG, Moon Larson M, Mattoon JS. Liver. In: Mattoon JS, Nyland TG (eds.): Small
298 Animal Diagnostic Ultrasound. 3rd ed. St Louis: Elsevier, 2015;348-399.
299 5. Guillot M, D'Anjou MA, Alexander K, Bedard C, Desnoyers M, Beauregard G, et al. Can
300 sonographic findings predict the results of liver aspirates in dogs with suspected liver
301 disease? Vet Radiol Ultrasound 2009;50:513-518.
302 6. Kemp SD, Panciera DL, Larson MM, Saunders GK, Werre SR. A comparison of hepatic
303 sonographic features and histopathologic diagnosis in canine liver disease: 138 cases. J Vet
304 Intern Med 2013;27:806-813.
305 7. Masserdotti C, Drigo M. Retrospective study of cytologic features of well-differentiated
306 hepatocellular carcinoma in dogs. Vet Clin Pathol 2012;41:382-390.
307 8. Nakamura K, Takagi S, Sasaki N, Bandula Kumara WR, Murakami M, Ohta H, et al.
308 Contrast-enhanced ultrasonography for characterization of canine focal liver lesions. Vet
309 Radiol Ultrasound 2010;51:79-85.
310 9. Fukushima K, Kanemoto H, Ohno K, Takahashi M, Nakashima K, Fujino Y, et al. CT
311 characteristics of primary hepatic mass lesions in dogs. Vet Radiol Ultrasound 2012;53:252-
312 257.
313 10. Kutara K, Seki M, Ishikawa C, Sakai M, Kagawa Y, Iida G, et al. Triple-phase helical
314 computed tomography in dogs with hepatic masses. Vet Radiol Ultrasound 2014;55:7-15.

315 11. Clifford CA, Pretorius ES, Weisse C, Sorenmo KU, Drobatz KJ, Siegelman ES, et al.
316 Magnetic resonance imaging of focal splenic and hepatic lesions in the dog. J Vet Intern Med
317 2004;18:330-338.
318 12.Huppertz A, Balzer T, Blakeborough A, Breuer J, Glovagnoni A, Heinz-Peer G, et al.
319 Improved detection of focal liver lesions at MR imaging: multicenter comparison of
320 gadoxetic acid-enhanced MR images with intraoperative findings. Radiology 2004;230:266-
321 275.
322 13. Van Beers BE, Pastor CM, Hussain HK. Primovist, Eovist: What to expect? J Hepatol
323 2012;57:421-429.
324 14. Leyendecker JR. Gadoxetate disodium for contrast magnetic resonance imaging of the
325 liver. Gastroenterol Hepatol. 2009;5:698.
326 15. Marks AL, Hecht S, Stokes JE, Conklin GA, Deanna KH. Effects of gadoxetate disodium
327 (Eovist®) contrast on magnetic resonance imaging characteristics of the liver in clinically
328 healthy dogs. Vet Radiol Ultrasound 2014;55:286-291.
329 16. Yonetomi D, Kadosawa T, Miyoshi K, Nakao Y, Homma E, Hanazono K, et al. Contrast
330 agent Gd-EOB-DTPA (EOB Primovist®) for low-field magnetic resonance imaging of
331 canine focal liver lesions. Vet Radiol Ultrasound 2012;53:371-380.
332 17. Louvet A, Duconseille AC. Feasibility for detecting liver metastases in dogs using
333 gadobenate dimeglumine-enhanced magnetic resonance imaging. Vet Radiol Ultrasound
334 2015;56:286-295.
335 18. Jia J, Puls D, Oswald S, Jedlitschky G, Kuhn JP, Weitschies W, et al. Characterization of
336 the intestinal and hepatic uptake/efflux transport of the magnetic resonance imaging contrast
337 agent gadolinium-ethoxylbenzyl-diethylenetriamine-pentaacetic acid. Invest Radiol
338 2014;49:78-86.

Plane	Flip Angle	TR	TE	NEX	Slice Thickness	FOV (row/column)	Matrix Size	Aver (

339 19. Wilby AJ, Maeda K, Courtney PF, Debori Y, Webborn PJH, Kitamura Y, et al. Hepatic
340 uptake in the dog: comparison of uptake in hepatocytes and human embryonic kidney cells
341 expressing dog organic anion-transporting polypeptide 1B4. Drug Metab Dispos
342 2011;39:2361-2369.
343 20. Ninomiya M, Ito K, Horie T. Functional analysis of dog multidrug resistance-associated
344 protein 2 (MRP2) in comparison with rat MRP2. Drug Metab Dispos 2005;33:225-232.
345 21. Kitao A, Matsui O, Yoneda N, Kozaka K, Shinmura R, Koda W, et al. The uptake
346 transporter OATP8 expression decreases during multistep hepatocarcinogenesis: correlation
347 with gadoxetic acid enhanced MR imaging. Eur Radiol 2011;21:2056-2066.
348 22. van Kessel CS, Veldhuis WB, van den Bosch MA, van Leeuwen MS. MR liver imaging
349 with Gd-EOB-DTPA: a delay time of 10 minutes is sufficient for lesion characterisation. Eur
350 Radiol 2012;22:2153–2160.
351 23. Fields EL, Robertson ID, Osborne JA, Brown JC. Comparison of abdominal computed
352 tomography and abdominal ultrasound in sedated dogs. Vet Radiol Ultrasound 2012;53:513-
353 517.
354 </BIBL>

355 Appendix 1. Magnetic Resonance Image Sequence Parameters

Dorsal	136-150	532-592	12	1-3	4-5 mm	320 x 240-272	320 x 218-231
Transverse	90	387-497	17	1-2	4-6 mm	408-512 x 408-512	256 x 153-192
Dorsal	150	2970-3800	100-103	1-3	4-5 mm	320 x 240-272	320 x 204-231
Transverse	122-150	3150-4850	82-87	1-2	4-6 mm	256-320 x 256-320	320 x 192-240
Dorsal	68	4.26-4.8	2.13-2.4	1-2	4-5 mm	256 x 200-216	256 x 150-162
Sagittal	68	4.3-4.8	2.15-2.4	1-2	5-6 mm	256 x 208	256 x 156
Transverse	10-31.7	3.66-5.08	1.47-2.39	1	1.5-3 mm	250-324 x 216-384	256-384 x 163-243
Transverse	10-31.7	3.66-5.08	1.54-2.39	1	2-3 mm	250-320 x 216-320	256-320 x 163-208
Dorsal	136-150	532-812	12	1-3	4-5 mm	320 x 208-320	320 x 177-272
Transverse	90	497-648	17	1	4-6 mm	512 x 408-464	256 x 153-174

TR, repetition time (in milliseconds, ms); TE, echo time (ms); NEX, number of excitations; TSE, turbo spin echo; SE, spin echo; VIBE, volume-interpolated body examination (T1-weighted 3D gradient echo sequence); W, weighted; TrueFISP, fast imaging with steady state precession.

Appendix 2. Signal Intensity of Confirmed Hepatocellular Carcinoma Lesions

Sequence	Hypointense Only	Isointense Only	Hyperintense Only	Hypointense & Isointense	Isointense & Hyperintense	Hypointense & Hyperintense
Pre-contrast T1-W SE	1/8 (12.5%)	1/8 (12.5%)	1/8 (12.5%)	2/8 (25%)	3/8 (37.5%)	n/a
T2-W TSE	n/a	1/8 (12.5%)	3/8 (37.5%)	n/a	2/8 (25%)	2/8 (25%)
TrueFISP	1/8 (12.5%)	n/a	1/8 (12.5%)	1/8 (12.5%)	2/8 (25%)	2/8 (25%)
Pre-contrast VIBE	2/8 (25%)	n/a	n/a	5/8 (62.5%)	n/a	1/8 (12.5%)

Post-contrast VIBE (all time points)	8/8 (100%)	n/a	n/a	n/a	n/a	n/a
Post-contrast T1-W Fat Sat	n/a	3/8 (37.5%)	3/8 (37.5%)	n/a	1/8 (12.5%)	1/8 (12.5%)

TSE, turbo spin-echo; VIBE, volume-interpolated body examination (T1-weighted 3D gradient echo sequence); W, weighted; TrueFISP, fast imaging with steady state precession.

FIGURE LEGENDS

Fig. 1. Transverse pre-contrast T1-W SE (A), transverse T2-W TSE (B), transverse pre-contrast T1-W GRE (C), transverse post-contrast T1-W GRE immediately (0) and at 1, 5, 10 and 20 minutes (D-H), and transverse 25 minute post-contrast T1-W FatSat (I) images in a 12 year-old neutered male Border Collie (patient 7) at the same level. (A) There is an irregular heterogeneous mass in the left ventral aspect of the liver (arrows) with an additional slightly hyperintense second mass in the right dorsal aspect of the liver (arrowheads). The gallbladder displays a layered appearance (asterisk). (B) The mass in the left ventral aspect of the liver is markedly heterogeneous (grade 3) with the smaller mass in the right dorsal aspect of the liver being mildly heterogeneous (grade 1). (C) The left-sided mass is similar to (A) with the right-sided mass being fairly inconspicuous. (D-H) There is progressive enhancement of the normal hepatic parenchyma (†) with the majority of both masses being hypointense at all time points. (I) The left-sided lesion remains heterogeneous with the periphery being slightly hyperintense. The right-sided lesion is homogeneous and hyperintense.

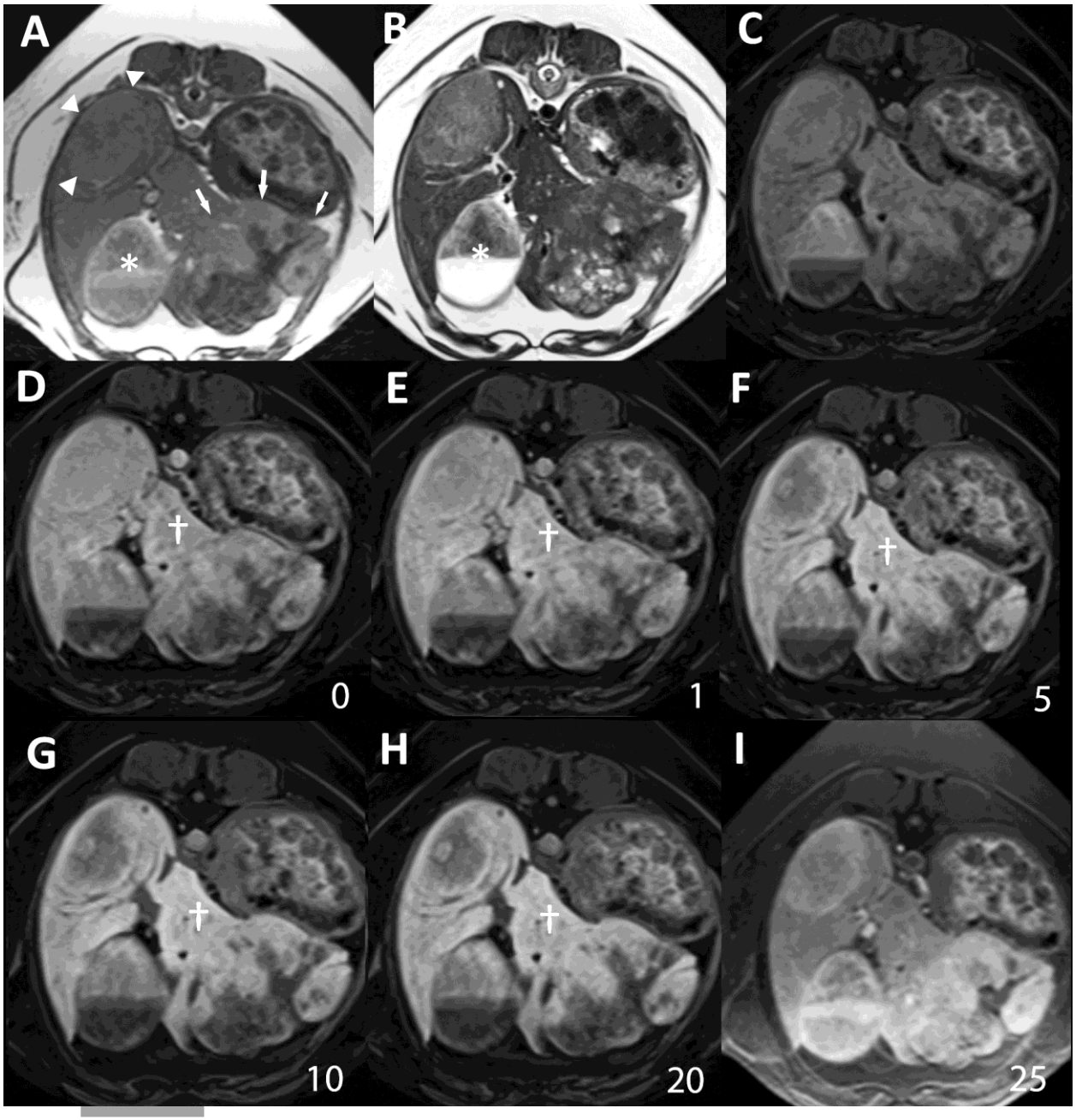

Fig. 2. Graphic representation of the signal intensity ratios (SIR) of the HCC lesions to normal hepatic parenchyma. Measurements were obtained before (pre), immediately (0), 1, 5, 10, and 20 min after intravenous administration of gadoxetate disodium. In the majority of cases, the lowest SIR values were reached at 10 minutes indicative of maximum difference between lesion and normal parenchymal enhancement. This time point marks the end of the wash-in period and start of the wash-out period.

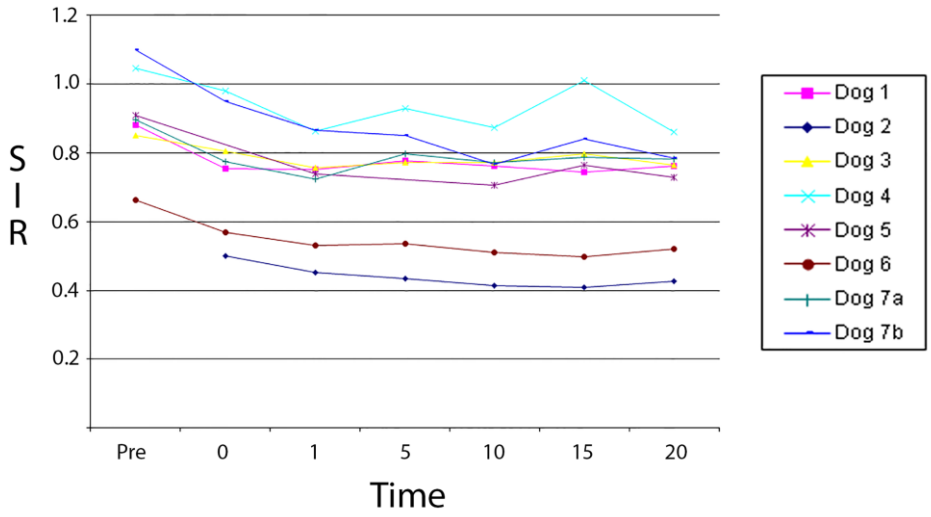

Fig. 3. Transverse T2-W TSE image (A) and transverse T1-W GRE image 10 minutes following contrast medium administration (B) in a 13 year old Boston Terrier (patient 1). A large mass originates from the papillary process of the quadrate lobe of the liver (asterisk). This lesion is T2 hypointense (A), mildly heterogeneous (grade 1), and shows decreased contrast medium uptake compared to normal liver parenchyma (B). Additionally, multiple faint T2 hypointense nodules are visible throughout the liver (A; arrows) which are not seen on the post contrast image (B), indicating similar contrast medium uptake compared to normal liver parenchyma. The liver was noted to be diffusely abnormal with multiple small nodules during surgery, and biopsies were obtained. Histopathology yielded a diagnosis of hepatocellular carcinoma for the hepatic mass and vacuolar hepatopathy for multiple liver nodules.

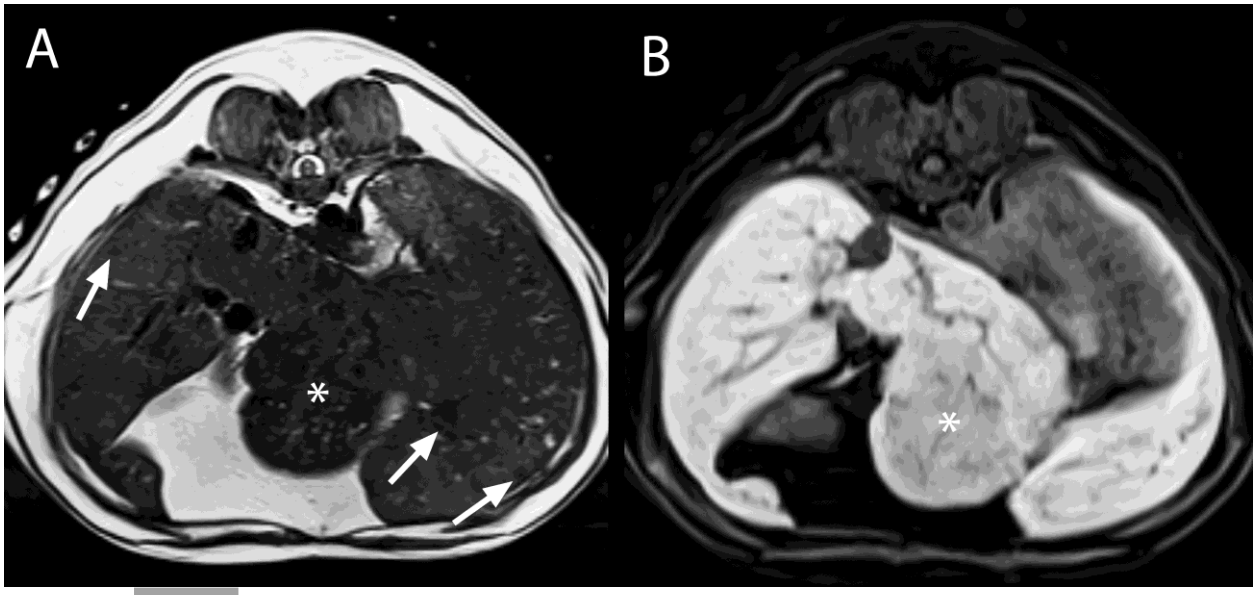

397

398

399